Ab Initio Calculations of Reactive Pathways for α-Octahydro-1,3,5,7-tetranitro-1,3,5,7-tetrazocine (α-HMX)

James P. Lewis,* Kurt R. Glaesemann, Kirk VanOpdorp, and Gregory A. Voth

Department of Chemistry and Henry Eyring Center for Theoretical Chemistry, University of Utah, 315 South 1400 East, Salt Lake City, Utah 84112-0850

Using the BLYP and B3LYP level of density functional theory, four possible decomposition reaction pathways of HMX in the gas phase were investigated: $N-NO_2$ bond dissociation, HONO elimination, $C-N$ bond scission of the ring, and the concerted ring fission. The energetics of each of these four mechanisms are reported. Dissociation of the $N-NO_2$ bond is putatively the initial mechanism of nitramine decomposition in the gas phase. Our results find the dissociation energy of this mechanism to be 41.8 kcal/mol at the BLYP level and 40.5 kcal/mol at the B3LYP level, which is comparable to experimental results. Three other mechanisms are calculated and found at the BLYP level to be energetically competitive to the nitrogen−nitrogen bond dissociation; however, at the B3LYP level these three other mechanisms are energetically less favorable. It is proposed that the HONO elimination and $C-N$ bond scission reaction of the ring would be favorable in the condensed phase.

I. Introduction

Cyclic aliphatic nitramines are important and widely used energetic materials. In particular, octahydro-1,3,5,7-tetranitro-1,3,5,7-tetrazocine (HMX) and hexahydro-1,3,5-trinitro-1,3,5-triazine (RDX) have become key materials for a variety of military and industrial applications due to their thermal stability and high detonation velocity relative to other explosives.[1,2] Because of their widespread use, a more rigorous investigation into their properties and their reactive mechanisms has become a contemporary topic of interest for experimentalists and theoreticians alike.

Although RDX and HMX have been used for military applications for over 50 years, scientific investigation into their reactive processes has only been undertaken in the past two decades. Significant progress has been made in understanding the microscopic nature of these explosives; however, fundamental questions remain unanswered. In particular, the time frame associated with explosive reactions in addition to the highly exothermic conditions associated with an explosion make experimental investigation of the initial steps of the reaction difficult at best. The primary motivation for this research is to use quantum chemistry techniques to complement current experimental investigations. Quantum chemistry techniques allow us the flexibility to explore time scales, temperature regimes and physical dimensions that are important to understanding the nature of this reactivity. Recent years have seen dramatic improvements in these methods that have resulted in their widespread use, not to mention a greater understanding of their range of applicability.

Several different studies of quantum chemistry calculations of nitramines have been previously reported. Density functional theory (DFT) has proven to be the most effective method for studying HMX and RDX due to the size of these respective molecules and the relative computational demands of the quantum chemistry methods used to study their reactive properties. Wu and Fried have employed DFT to investigate the reactive properties of RDX in the gas phase.[3] In particular, they calculated the potential energy surface along a single reaction coordinate for $N-NO_2$ bond dissociation and concerted symmetric ring fission to three $CH_2N_2O_2$ molecules. Harris and Lammertsma likewise invesitgate the $C-H$ bond dissociation in RDX and find it energetically unfavorable compared to $N-NO_2$ bond dissociation.[4] Additionally, Manaa and Fried used DFT to calculate the singlet and triplet states of the carbon−nitrogen dissociation in nitromethane and compared those results to multiconfiguration self-consistent field (MCSCF) and quadratic configuration interaction (QCI) ab initio calculations.[5] Rice and co-workers have also employed DFT methods to study the behavior of nitramines in two comparisons of density functional methods with higher level quantum chemistry methods.[6,7] In their first study, Pai it et al. compared the performance of various DFT functionals with various basis sets to the performance of MP2 for the potential energy surface of sym-Triazine reactions.[6] In their second study, they employed the same two types of calculations in examining the structure and relative stability of conformers of RDX.[7] More recently, Chakraborty et al. performed DFT calculation to map out several transition states for RDX.[8]

Despite the numerous theoretical results for RDX, very few theoretical results have been reported for HMX. Recently, we used a local-orbital DFT approach to study the energetics and structures of the three pure polymorphic forms of crystalline HMX.[9] In this work, the energetics of four possible reaction mechanisms of HMX are investigated: $N-NO_2$ bond dissociation, HONO elimination, $C-N$ bond dissociation of the ring, and the concerted ring fission to four $CH_2N_2O_2$ molecules. It is important to note that despite the report of similar calculations for RDX, there are differences in the decomposition environments of HMX and RDX[10,11] including evidence that HMX decomposes in the solid phase[12] as opposed to the liquid-phase decomposition of RDX. These differences often depend on the various experimental conditions under which the experiments are performed. In this paper, we pursue calculations to inves-

Reactive Pathways for α-HMX

J. Phys. Chem. A, Vol. 104, No. 48, 2000 **11385**
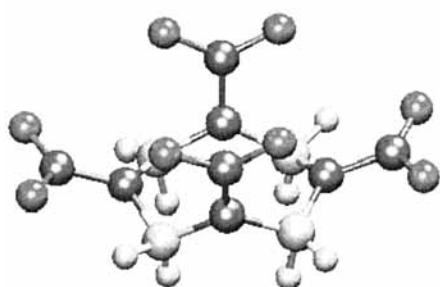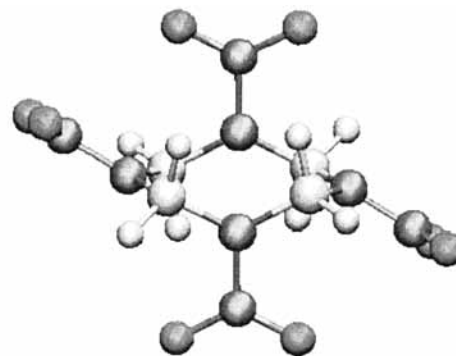
Figure 1. Boat and chair gas-phase conformers of HMX.

tigate these four reaction mechanisms of HMX in order to further understand decomposition pathways that are specific to HMX.

The sections of this paper are organized as follows: The computational methods are described in section II, while section III discusses some background information on HMX as well as a comparison of calculations for the two different conformers. Section IV discusses the result of the calculations for the four different reaction mechanisms described above. Finally, section V contains some concluding remarks.

II. Computational Methods

All of the energy calculations presented herein were performed using the Gaussian98[13] quantum chemistry package on a Silicon Graphics Origin 2000 computer. Within this package, the Kohn−Sham spin unrestricted DFT formulation was employed[14,15] and the spin state was initially contaminated with a mixed singlet−triplet state. The local-density approximation (LDA) of DFT has proven to be highly unreliable for predicting dissociation energies;[16−19] therefore, we use the generalized-gradient approximation (GGA) of DFT. It has been demonstrated that GGAs yield a level of accuracy comparable to other sophisticated ab initio methods.[17,18,20,21] In addition, the favorable scaling of DFT methods with system size compared to other high-level quantum chemistry methods makes them more desirable to use for larger systems such as HMX.

Two gradient-corrected functionals were chosen for this study: BLYP and B3LYP. The Becke gradient-corrected exchange functional (B) has been shown to reproduce the exact asymptotic behavior of exchange energy density in a finite system.[22,23] The Becke three-parameter exchange (B3) is a hybrid method that mixes some Hartree−Fock exchange energy into the exchange functional.[24] This mixing is shown to improve the barrier height of some reactions which may normally be underestimated due to the Coulomb *self-interaction* of the electrons.[19,21,25,26] The correlation functional used is the gradient-corrected functional of Lee, Yang, and Parr (LYP).[27] Previous work shows that these two methods can properly describe the complete dissociation curve using spin-unrestricted formulations.[18,28] Additionally, Wu and Fried demonstrated that these two functionals yield good results for RDX, which is similar in composition to HMX.[3]

The basis set used in this study was 6-311G with additional p-functions for H and additional d-functions for the second row elements: C, N, and O. These calculations were carried out at 0 K, and as a result the several high-frequency modes attributable to carbon−hydrogen stretch modes may contribute a significant zero-point vibrational energy. Therefore, a zero-point

TABLE 1: Relative Energies (kcal/mol), Bond Lengths (Å), and Bond Angles (deg) of the Boat and Chair Conformations of HMX[a]

	chair (BLYP)	boat (BLYP)	chair (B3LYP)	boat (B3LYP)
relative energy	0.00	0.81	0.00	2.33
av bond lengths				
N−N (equatorial)	1.46	1.43	1.39	1.41
N−N (axial)	1.45	1.44	1.40	1.42
N−O	1.23	1.23	1.22	1.22
C−N	1.47	1.47	1.46	1.45
H−C	1.10	1.10	1.09	1.09
av bond angles				
N−N−O	116.27	116.21	116.44	116.51
O−N−O	127.47	127.51	127.08	126.98
C−N−N	117.06	116.89	117.38	117.69
C−N−C	122.67	122.89	123.22	122.75
N−C−H	108.05	108.67	108.79	108.27

[a] Results were obtained with both the BLYP and B3LYP levels of density-functional theory.

energy (ZPE) correction was included in the total energy calculations for each optimized geometry.[13]

III. HMX Background

The HMX molecule is an eight-membered ring of alternating carbon and nitrogen atoms, where two hydrogen atoms are bonded to each carbon atom and a nitro group is bonded to each nitrogen atom. There are four polymorphs of HMX: α, β, δ, and γ, with the β polymorph (chair conformation) as the room-temperature stable form.[29] The α and δ polymorphs (boat conformations) are stable from approximately 377 to 429 K and approximately 429 to 549K (melting point), respectively.[30,31] The γ polymorph is a metastable hydrated structure (stable at approximately 429 K) that converts immediately to β-HMX in the presence of solvent.[32,33]

In the gas phase there are two stable structural conformers of HMX: the boat form and the chair form (see Figure 1). Starting from the initial X-ray crystallographically determined structures of α-, β-, and δ-HMX, calculations were performed using the methods described in section II. It was found that the α and δ structures both optimize to the boat conformer and β-HMX optimizes to the chair conformer. The relative energies and geometries of the two conformationally different structures are listed in Table 1. The boat conformation is higher in energy than the chair conformation by 0.81 kcal/mol (BLYP) and 2.33 kcal/mol (B3LYP). It is interesting to note that the bond lengths and angles of the two structures are virtually indistinguishable, which perhaps explains their closeness in energy. However, there are significant differences between the BLYP structures and the

SCHEME 1
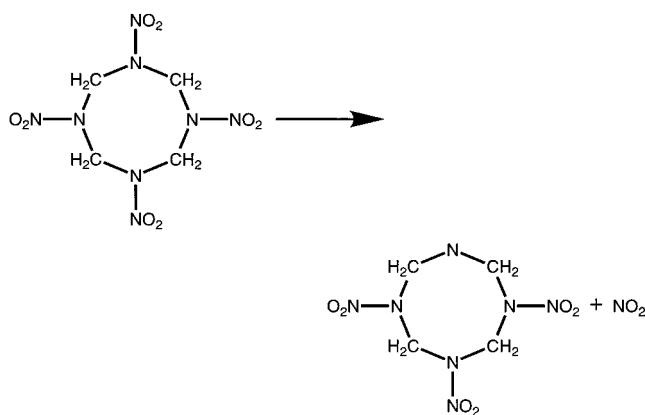
SCHEME 2
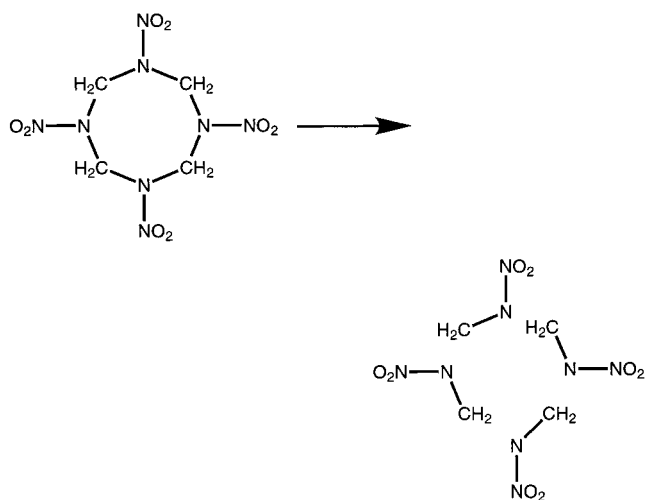
B3LYP structures; the former yields larger N−N bond lengths in both the equatorial and axial directions.

Four different unimolecular reaction mechanisms for HMX were investigated: dissociation of NO_2, concerted ring scission, elimination of HONO, and dissociation of the ring along the C−N bond. Among these several mechanisms, the putative initial mechanism for decomposition of nitramines is the rupture of the N−NO_2 bond (Scheme 1).

Through transient laser pyrolysis experiments, Wight and Botcher have shown that in RDX the initial decomposition products involve the removal of a single NO_2.[34−36] Their experiments were performed using a solid thin film; therefore, it appears that the N−NO_2 bond dissociation occurs more abundantly as a result of the large surface exposure of the NO_2 groups. In addition to these experiments, dissociation NO_2 is also proposed as a primary decomposition pathway under collisionless, infrared multiphoton dissociation (IRMPD) experiments.[37]

In addition to the dissociation of the NO_2 bond, these IRMPD experiments propose that two other competing mechanisms exist in RDX: concerted ring fission of RDX into three $CH_2N_2O_2$ molecules and elimination of HONO from the molecule. Similarly, we investigate concerted ring fission of HMX into four $CH_2N_2O_2$ molecules (Scheme 2) and HONO elimination from HMX (Scheme 3).

Earlier DFT results for RDX in the gas phase demonstrated that N−NO_2 bond dissociation is more energetically favorable (∼18 kcal/mol) over concerted ring fission.[3] The products that may be produced from either of these mechanisms are supported

SCHEME 3
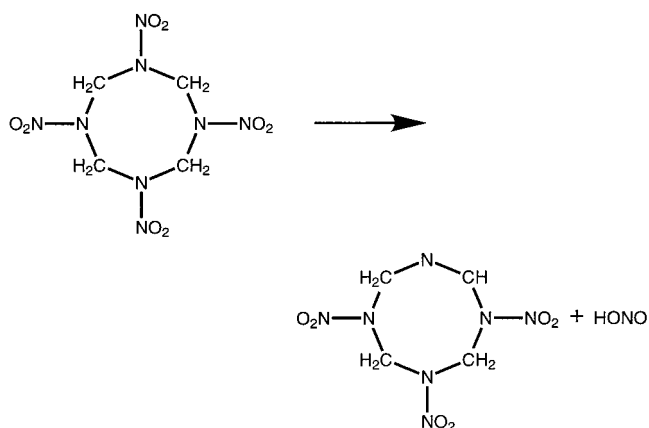
from experimental evidence where gaseous pyrolysis products were examined from the thermal decomposition of HMX.[10−12,38,39] Elimination of HONO is proposed as either a primary or secondary mechanism; however, only the primary reaction mechanism is investigated in this work.

HMX decomposition is known to occur under different conditions than RDX; the former decomposes in a condensed-phase environment rather than a gas-phase environment. It is commonly thought that the confining environment of a condensed phase would provide more steric constraints which prohibit a mechanism such as the ring fission reaction from proceeding.[34,36] Moreover, condensed phase experiments are difficult to interpret because several possible product species can be created. As a result, we also investigated a mechanism not previously proposed—scission of the ring via a C−N bond. Preliminary results of condensed-phase calculations suggest that this mechanism as well as HONO elimination may be energetically more favorable than N−NO_2 dissociation in a condensed-phase environment due to the steric hindrance of the latter in the solid state.[9]

Although HMX decomposes in the condensed phase, the current results presented here are results from calculations in the gas phase. Understandably, the energetics of these calculations will not exactly predict the true energetic pathway in the condensed-phase environment. However, these results will be used as first-order approximations for later studies of viable condensed-phase reaction mechanisms.

IV. Results

A. N−N Bond Scission. Using the BLYP and B3LYP level of DFT in Gaussian98, the N−N bond scission energy for HMX in the gas phase was calculated. For a given range of fixed N−N bond lengths, the structure of HMX was optimized. The α and δ forms of HMX (boat conformation) are the higher temperature structures, from which the decomposition of HMX occurs; hence, this form was used to generate the calculated data. Figure 2 shows a plot of the energy (BLYP and B3LYP), including the ZPE, as a function of this bond length. As shown in the data, there is no barrier to dissociation in the gas phase, suggesting that N−NO_2 bond cleavage in condensed-phase HMX is a highly reversible process.

From these results, we find that the N−NO_2 bond dissociation energy is 41.8 kcal/mol at the BLYP level and 40.5 kcal/mol at the B3LYP level. The potential energy profile value compares extremely well with the N−N bond scission energy curves for RDX determined both theoretically and experimentally. Previous calculations of the RDX found that the dissociation energy for
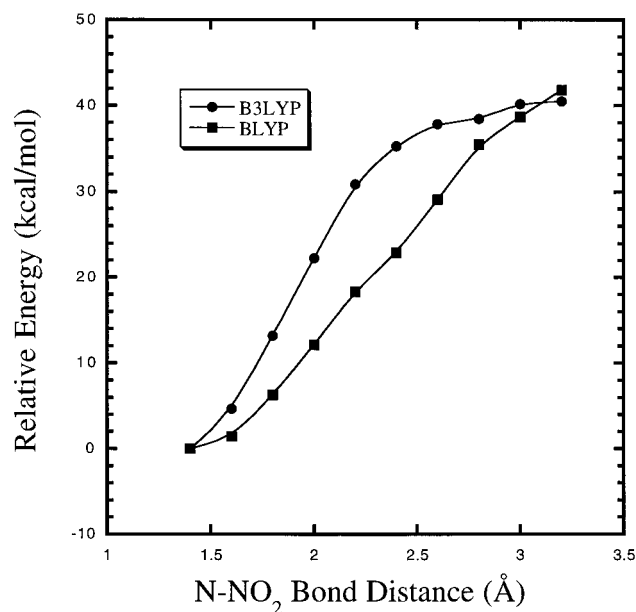
Reactive Pathways for α-HMX

J. Phys. Chem. A, Vol. 104, No. 48, 2000 **11387**

Figure 2. Energy versus equatorial N−N bond length for the boat conformation of HMX.

Figure 3. Energy versus C−N bond length (concerted scission) for the boat conformation of HMX.

the rupture of the N−NO₂ bond ranges between 38.7 and 43.4 kcal/mol for different levels of theory.[3] Likewise, recent experimental results of RDX have yielded an estimated activation barrier for the initial decomposition step as ∼37 kcal/mol.[40] Although these experimental estimates may not represent the energy of N−N bond scission, microscopic imaging of the decomposed crystal suggests that this is the decomposition mechanism at work. Finally, the potential energy profile shown in Figure 2 has zero barrier, which is in agreement with experimental observations which indicate that the product translational energy distribution for the N−NO₂ cleavage is peaked at zero.[37] Therefore, this mechanism is likely reversible in the condensed phase.

B. Concerted Symmetric Ring Fission. In this proposed reaction mechanism, the molecule decomposes into four CH₂N₂O₂ molecules (see Scheme 2). Each fragment then undergoes a proposed secondary decomposition reaction yielding experimentally observed products: HCN, HONO, N₂O, and H₂CO. Calculations were performed for fixed C−N distances on the ring; the geometry for each fixed C−N distance was optimized. Figure 3 shows a plot of the energy (BLYP and B3LYP), including the ZPE, as a function of this distance.

Unlike dissociation of NO₂ from the molecule, a definite barrier exists between the ground state structure and the stable intermediate formed as the fragments become segregated. This barrier between the ground state and the stable intermediate (formed when the fragments are further apart) is found to be approximately 48.1 kcal/mol at the BLYP level and 71.8 kcal/mol at the B3LYP level. Therefore, this process would not be reversible in the condensed phase as observed for the case of NO₂ dissociation. The energy of this barrier relative to the dissociation energy of the N−NO₂ bond rupture is less favorable by approximately 6.3 kcal/mol (BLYP) and 31.8 kcal/mol (B3LYP). Spin-restricted calculations yielded very similar results, and similar results were reported for DFT calculations of RDX.[3]

The intermediate produced from the concerted ring fission is calculated to be more favorable than the N−NO₂ bond dissociation (for both BLYP and B3LYP); however, the formation of this intermediate occurs at relatively large C−N distances. In the condensed phase, the packing of the molecules
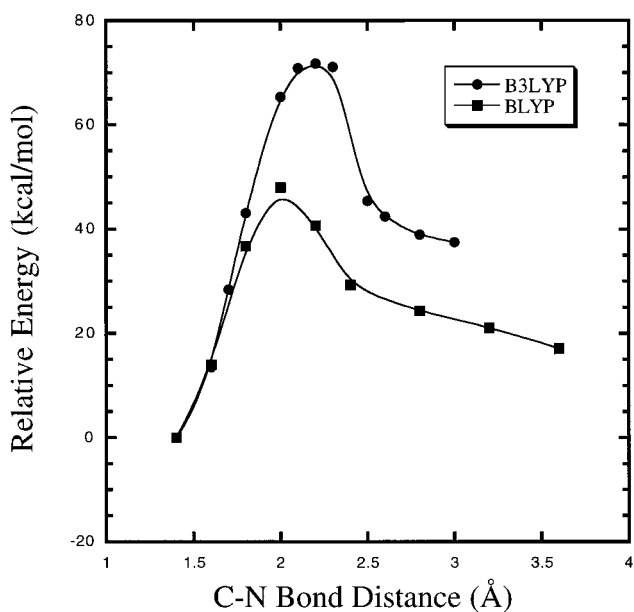
would produce a steric constraint that would likely inhibit formation of this intermediate. This physical constraint, in combination with the relatively large barrier for the concerted ring fission, implies that this reaction mechanism is very unlikely in an ideal crystalline condensed-phase environment. The probability of this mechanism occurring would perhaps increase if vacancies or cavities were to form in the molecular crystal. These cavities would remove some of the physical constraints that exist, allowing the concerted ring fission to proceed as a possible mechanism.

C. HONO Elimination. The transition-state searching algorithm within Gaussian98 was used to determine a transition state for elimination of HONO from the HMX molecule (see Scheme 3). A transition state using the BLYP level of DFT was found yielding a barrier between the ground state and product state. The energy of this transition-state barrier is 42.9 kcal/mol (BLYP), which is quite comparable to the amount of energy required for dissociation of NO₂ from the molecule.

With a barrier comparable to NO₂ dissociation and an energetically favorable intermediate, this reaction mechanism appears quite competitive to the putatively accepted primary decomposition pathway. One advantage for this mechanism is that it forms the stable intermediate and is not reversible in the condensed phase. Therefore, this reaction mechanism is more likely to encourage further secondary decomposition of HMX in the condensed phase; whereas, NO₂ dissociation may not because no stable intermediate is formed in the latter. In addition, the HONO elimination pathway is not as sterically confined by the molecular environment as the NO₂ dissociation and the concerted ring scission pathways.

D. C−N Bond Scission. The potential energy curve corresponding to C−N bond scission was calculated by optimizing the HMX geometry for several C−N bond distances. The potential energy curve calculated represents optimization along a specific energetic pathway corresponding to fixed C−N bond lengths and not optimization to a saddle point. The results of these calculations indicate that the barrier for this specific C−N bond elongation pathway is 41.2 kcal/mol at the BLYP level and 56.0 kcal/mol at the B3LYP level. These energy barriers are comparable to the calculated energy of the putatively favored
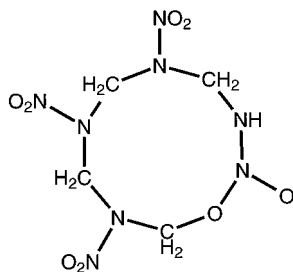
11388 *J. Phys. Chem. A, Vol. 104, No. 48, 2000*

Lewis et al.

Figure 4. Ten-membered ring intermediate structure of HMX.

Figure 5. Proposed reaction products of the ten-membered ring intermediate of HMX.

N−NO₂ bond dissociation. These results represent only an upper bound for the C−N bond scission reaction pathway; further investigations will determined a more accurate energy profile for this mechanism in a condensed phase.

In the process of optimizing the structure for each C−N bond distance, our calculations find that the energy increases as this distance increases, as expected. The energy peaks, and then beyond some energetic barrier a stable 10-membered ring intermediate, schematically shown in Figure 4, is formed. The energy of this intermediate is found to be only 10.3 kcal/mol (BLYP) and 11.5 kcal/mol (B3LYP) above the ground-state gas-phase HMX molecule. As with the HONO elimination this mechanism would not be reversible in the condensed phase at the formation of this stable intermediate. More importantly, the intermediate formed is the most energetically favorable of the four proposed mechanisms.

The results presented here indicate that the C−N bond scission barrier is only somewhat less energetically favorable (at the B3LYP level) compared to N−NO₂ bond dissociation. It is important to note that these calculations have been performed in the gas phase and condensed-phase effects may change, even reverse, the relative energy ordering of the barriers. The relatively compact structure of the C−N bond scission transition state may be structurally less confining compared to the drastic extension of the N−N bond that must take place for the NO₂ group to dissociate. Preliminary condensed-phase calculations of the potential energy surface in our group indicate that in the compact crystal structure N−N bond dissociation is energetically discouraged compared to the C−N bond scission mechanism. Of course, near areas with large surfaces or voids there is no confining environment and N−N bond dissociation would likely be more favorable.

This work represents the first determination of an intermediate for the C−N bond scission. Although such an intermediate has never before been proposed, the experimental data available to us regarding the gaseous products formed during HMX decomposition support such an intermediate. In particular, Behrens has shown that the three primary decomposition products are N₂O, H₂O, and CH₂O.[12,10] While the intermediate proposed here does not address the formation of H₂O, it is a plausible explanation for the abundance of both N₂O and CH₂O. Behrens explains the formation of such products through a two-step process involving an initial N−N bond scission forming NO₂ and H₂CN, which recombine to form N₂O and CH₂O. While this is still plausible, the abundance of the N₂O and CH₂O products would point to a primary decomposition mechanism that results in these products. Clearly, the simple fragmentation of the intermediate proposed here would fit that description, as shown in Figure 5.

Additionally, Behrens isotopically labeled decomposition experiments also indicate that very little ¹⁵N−¹⁴N mixing (<5%) and H−D mixing (<7%) occurs in N₂O and CH₂O, respectively. Th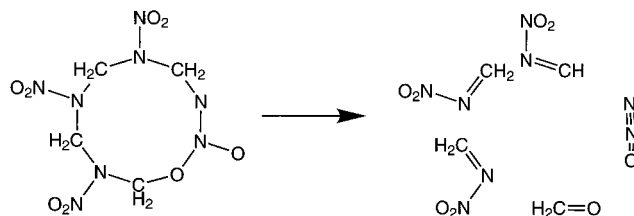is would indicate that N₂O originates directly from the ring and not via N−N bond breaking. The lack of H−D mixing would also seem to indicate that CH₂O originates directly from the ring. Behrens does observe a large amount (≈80%) of ¹³C−¹²C and ¹⁸O−¹⁶O scrambling in the CH₂O product. However, it is important to note that in a high-temperature experiment such as this, isotopic exchange can occur during the initial reaction or during secondary reactions prior to detection. Consequently, the lack of isotopic scrambling is more positive proof but the existence of isotopic scrambling is inconclusive. Behrens points out specifically that carbon and oxygen scrambling could likely occur during the formation and subsequent decomposition of a formaldehyde polymer or during an aldehyde hydration/dehydration process.

Although the fact that the experimental information is consistent with the intermediate in Figure 4, it certainly does not prove its existence nor its relevance to a condensed-phase reaction mechanism. However, this reaction mechanism is more likely to encourage further secondary decomposition of HMX in the condensed phase similar to HONO elimination. More conclusive evidence can be obtained from explicit condensed-phase reaction studies currently underway.

V. Concluding Remarks

As the scientific effort to understand the reactivity of highly energetic materials grows, quantum chemistry methods can play a useful role in that investigation. Because of the highly exothermic nature of explosive materials, it is difficult to investigate many aspects of their reactivity with current experimental techniques. However, quantum chemistry methods offer a risk-free and relatively accurate means by which to study their behavior.

On the basis of the gas-phase calculations reported in this paper, N−NO₂ bond dissociation, HONO elimination, and the proposed C−N bond scission are energetically comparable at the BLYP level: 41.8, 42.9, and 41.2 kcal/mol, respectively. The concerted ring scission of the HMX molecule into four CH₂N₂O₂ molecules is calculated to be less energetically favorable at both the BLYP and B3LYP levels. At the B3LYP level the proposed C−N bond scission is less favorable than N−NO₂ bond dissociation by 16.0 kcal/mol; however, the predicted intermediate is only approximately 10.0 kcal/mol above the ground-state gas-phase HMX structure. In a bulk condensed-phase environment the C−N bond scission mechanism may be energetically favored because of the steric constraints that will disfavor N−NO₂ bond dissociation. Further calculations of these mechanisms to understand the effects of the condensed-phase environment are underway. The uniquely identified intermediate of the C−N bond scission may play a role in the decomposition under certain experimental conditions in the condensed phase.

References and Notes

(1) Cooper, P. W.; Kurowski, S. R. *Introduction to the Technology of Explosives*; Wiley: New York, 1996.

(2) Akhaven, J. *The Chemistry of Explosives*; Royal Society of Chemistry: Cambridge, U.K., 1998.

(3) Wu, C. J.; Fried, L. E. *J. Phys. Chem. A* **1997** *101,* 8675.

(4) Harris, N. J.; Lammertsma, K. *J. Am. Chem. Soc.* **1997**, *119,* 6583.

(5) Manaa, M. R.; Fried, L. E. *J. Phys. Chem. A* **1999**, *102,* 9884.

(6) Pai, S. V.; Chabalowski, C. F.; Rice, B. M. *J. Phys. Chem.* **1996**, *100*, 15368.

(7) Rice, B. M.; Chabalowski, C. F. *J. Phys. Chem. A* **1997** *101,* 8720.

(8) Chakraborty, D.; Muller, R. P.; Dasgupta, S.; Goddard, W. A. *J. Phys. Chem. A* **2000,** *104,* 2261.

(9) Lewis, J. P.; Sewell, T. D.; Evans, R. B.; Voth, G. A. *J. Chem. Phys. B* **2000,** *104,* 1009.

(10) Behrens, R.; Bulusu, S. *J. Phys. Chem.* **1991**, *95,* 5838.

(11) Behrens, R.; Bulusu, S. *J. Phys. Chem.* **1992**, *96,* 8877.

(12) Behrens, R. *J. Phys. Chem.* **1990**, *94,* 6706.

(13) Frisch, M. J.; Trucks, G. W.; Schlegel, H. B.; Scuseria, E.; Robb, M. A.; Cheeseman, J. R.; Zakrzewski, V. G.; Montgomery, J. A., Jr.; Stratmann, R. E.; Burant, J. C.; Dapprich, S.; Millam, J. M.; Daniels, A. D.; Kudin, K. N.; Strain, M. C.; Farkas, O.; Tomasi, J.; Barone, V.; Cossi, M.; Cammi, R.; Mennucci, B.; Pomelli, C.; Adamo, C.; Clifford, S.; Ochterski, J.; Petersson, G. A.; Ayala, P. Y.; Cui, Q.; Morokuma, K.; Malick, D. K.; Rabuck, A. D.; Raghavachari, K.; Foresman, J. B.; Cioslowski, J.; Ortiz, J. V.; Stefanov, B. B.; Liu, G.; Liashenko, A.; Piskorz, P.; Komaromi, I.; Gomperts, R.; Martin, R. L.; Fox, D. J.; Keith, T.; Al-Laham, M. A.; Peng, C. Y.; Nanayakkara, A.; Gonzalez, C.; Challacombe, M.; Gill, P. M. W.; Johnson, B.; Chen, W.; Wong, M. W.; Andres, J. L.; Gonzalez, C.; Head-Gordon, M.; Replogle, E. S.; Pople, J. A. *Gaussian 98*, Revision A.6; Gaussian, Inc.: Pittsburgh, PA, 1998.

(14) Hohenberg, P.; Kohn, W. *Phys. Rev.* **1964**, *136,* 864B.

(15) Kohn, W.; Sham, L. J. *Phys. Rev.* **1965**, *140,* 1133A.

(16) Kohn, W.; Becke, A. D.; Parr, R. G. *J. Phys. Chem.* **1996**, *100*, 12974.

(17) Fan L.; Zeigler, T. *J. Am. Chem. Soc.* **1992**, *114,* 10890.

(18) Andzelm, J.; Sosa, C.; R. A. Eades, R. A. *J. Phys. Chem.* **1993**, *97,* 4664.

(19) Johnson, B. G.; Gonzales, C. A.; Gill, P. M. W.; Pople, J. A. *Chem. Phys. Lett.* **1994** *221,* 100.

(20) Scuseria, G. E. *J. Chem. Phys.* **1992,** /em 97, 7528.

(21) Andzelm, J.; Baker, J.; Scheiner, A.; Wrinn, M. *Int. J. Quantum Chem.* **1995**, *56,* 733.

(22) Becke, A. D. *Phys. Rev. A* **1988**, *38,* 3098.

(23) Becke, A. D. *J. Chem. Phys.* **1993**, *98,* 5648.

(24) Hertwig, R. H.; Kohn, W. *Chem. Phys. Lett.* **1997**, *268,* 345.

(25) Baker, J.; Andzelm, J.; Muir, M. *J. Chem. Phys.* **1995**, *102,* 2063.

(26) Durant, J. L. *Chem. Phys. Lett.* **1996**, *256,* 595.

(27) Lee, C.; Yang, W.; Parr, R. G. *Phys. Rev. B* **1988**, *37,* 785.

(28) Andzelm, J.; Wimmer, E. *J. Chem. Phys.* **1992**, *96,* 1280.

(29) Choi, C. S.; Boutin, H. P. *Acta Crystallogr. B* **1970**, *26,* 1235.

(30) Cady, H. H.; Larson, A. C.; Cromer, D. T. *Acta Crystallogr.* **1963**, *16,* 617.

(31) Cobbledick, R. E.; Small, R. W. H. *Acta Crystallogr.* **1974**, *30,* 1918.

(32) Main, P.; Cobbledick, R. E.; Small, R. W. H. *Acta Crystallogr.* **1974** *C41,* 1351.

(33) Boggs, T. L. In *Fundamentals of Solid-Propellant Combustion*; Kuo K. K., Summerfield, M., Eds.; American Institute of Aeronautics and Astronautics, Inc.: Boston, 1984; p 121.

(34) Wight, C. A.; Botcher, T. R. *J. Am. Chem. Soc.* **1992**, *114,* 8303.

(35) Botcher, T. R.; Wight, C. A. *J. Phys. Chem.* **1994,** 97, 9149.

(36) Botcher, T. R.; Wight, C. A. *J. Phys. Chem.* **1994**, *98,* 5541.

(37) Zhao, X. S.; Hintsa, E. J.; Lee, Y. T. *J. Chem. Phys.* **1988**, *88,* 801.

(38) Behrens, R. In *Chemistry and Physics of Energetic Materials*; Bulusu, S. N., Ed.; Kluwer: Dordrecht, The Netherlands, 1989; p 347.

(39) Behrens, R.; Bulusu, S. *J. Phys. Chem.* **1992**, *96,* 8891.

(40) Lofy, P. A. Ph.D. Thesis, Department of Chemistry, University of Utah, Salt Lake City, Utah, 1999.